Hybrid Wing-Body Pressurized Fuselage and Bulkhead, Design and Optimization

Vivek Mukhopadhyay[1]
NASA Langley Research Center, Hampton, Virginia, 23681-2199

The structural weight reduction of a pressurized Hybrid Wing-Body (HWB) fuselage is a serious challenge. Hence, research and development are presently being continued at NASA under the Environmentally Responsible Aviation (ERA) and Subsonic Fixed Wing (SFW) projects in collaboration with the Boeing Company, Huntington Beach and Air Force Research Laboratory (AFRL). In this paper, a structural analysis of the HWB fuselage and bulkhead panels is presented, with the objectives of design improvement and structural weight reduction. First, orthotropic plate theories for sizing, and equivalent plate analysis with appropriate simplification are considered. Then parametric finite-element analysis of a fuselage section and bulkhead are conducted using advanced stitched composite structural concepts, which are presently being developed at Boeing for pressurized HWB flight vehicles. With this advanced stiffened-shell design, structural weights are computed and compared to the thick sandwich, vaulted-ribbed-shell, and multi-bubble stiffened-shell structural concepts that had been studied previously. The analytical and numerical results are discussed to assess the overall weight/strength advantages.

Nomenclature

a	=	spacing between y-directional stringer or frame.
A	=	beam column cross section area.
A_{sx}	=	section area of single x-directional frame or stringer.
A_{sy}	=	area of single y-directional stringer or frame.
b	=	spacing between x-directional frame or stringer.
B	=	total breadth of stiffened panel between end supports.
D	=	bending rigidity of plate $Et^3/12(1-\nu^2)$.
D_x	=	bending rigidity of stiffened orthotropic plate about the y axis.
D_y	=	bending rigidity of stiffened orthotropic plate about the x axis.
E_x, E_y	=	Young's modulus of orthotropic plate in x and y directions.
F_{cx}, F_{cy}	=	yield stress in compression along x and y directions.
F_{tx}, F_{ty}	=	yield stress in tension along x and y directions.
G	=	shear modulus.
H	=	$\sqrt{D_x D_y}$.
I	=	area moment of inertia for beam bending about neutral axis.
I_x, I_y	=	area moment of inertia of x- and y-stiffeners about neutral axis.
L	=	total length of stiffened panel between end supports.
ν_x, ν_y	=	Possion's ratio along x and y axis.
M_x, M_y	=	running bending moments about x and y axis, respectively (lb-inch/inch).
N_x, N_y	=	running in-plane load along x and y directions, respectively (lb./inch).
P_c	=	compression load on beam-column.
P_{cr}	=	compression buckling load on beam-column.
P	=	cabin pressure of 9.2 psi ($2P$ = 18.4 psi).
q	=	running normal load on beam or pressure on plate.
t	=	shell or skin thickness.
w	=	beam or plate deflection at mid-point.
x, y	=	x and y reference axes of the plate, respectively.
z	=	normal distance from beam or plate neutral plane.
Z_{ox}, Z_{oy}	=	neutral axis location of x- and y-stiffeners from skin mid plane.

[1] Senior Aerospace Engineer, Aeronautical Systems Analysis Branch, MS 442, AIAA Associate Fellow. (AIAA-Paper 2013-xxxx, 54th AIAA/ASME/ASCE/AHS/ASC SDM Conference, Boston, MA, April 2013)

I. Introduction

Design of efficient pressurized fuselage configurations for the Hybrid-Wing-Body[1-3] (HWB) and Advanced Mobility Concept[4] (AMC-X) flight vehicles are challenging opportunities for the efficient structures technology development. The stiffened cylindrical cross-section fuselage of Boeing 777 and 787, shown in figure 1, are quite efficient, since, when pressurized, the skin is mostly under tensile membrane stress. The Airbus A380 has an elliptic egg shaped cross-section which is strengthened by the twin deck floor beams. However, in a HWB fuselage with rectangular cross-section, the internal cabin pressure combined with flight loads primarily result in highly non-linear bending stress and large deformation. It can be shown[5-6] that these bending stresses are theoretically one order of magnitude higher than the membrane-hoop stress in a conventional cylindrical fuselage of similar size and skin thickness. Moreover, resulting deformation of the outer aerodynamic surface could significantly affect performance advantages provided by the large lifting body. Thus, it is necessary to design an efficient fuselage structure in order to reduce the overall structural deflection and weight penalty, while satisfying the design stress, strain, and buckling safety factors, under the critical design loads[7-10]. Many structural concepts such as the conventional skin-stringer-frame, ribbed-double-shell, multi-bubble stiffened shell, thick sandwich, J-Frame, Beaded-Hat, and stitched sandwich frame composite construction have been studied under AFRL and NASA research projects[8-10]. These concepts are schematically shown in Figure 1.

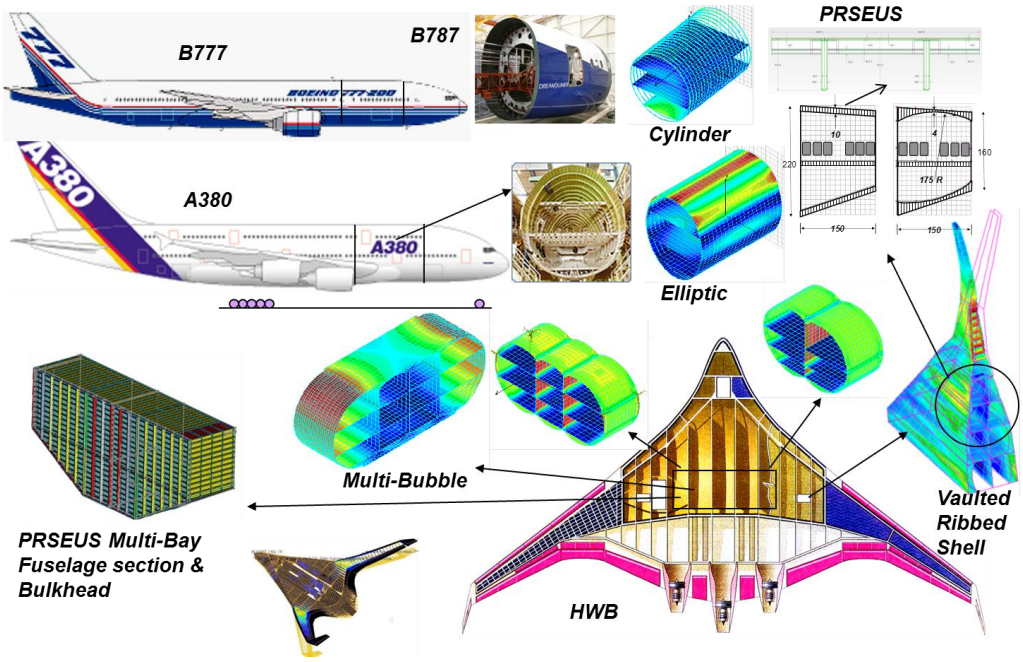

Figure 1. Fuselage section concept analysis models of B777, A380 and HWB class of vehicles.

A highly innovative advanced technology acronymed PRSEUS (Pultruded Rod Stitched Efficient Unitized Structure) is being developed at Boeing Phantom Works, with application to the pressurized HWB vehicles[11-16]. This involved analysis, design, fabrication and testing of PRSEUS coupons, panels and fuselage components, under the NASA Environmentally Responsible Aviation (ERA) Program's Airframe Technology subtask for structural weight and risk reduction. This development process [17-18] for the PRSEUS concept is schematically shown in Figure 2. Some initial results at the coupon, panel and fuselage section under one critical overpressure load condition were presented in Ref. 18. This paper will discuss additional analytical and numerical results of parametric design studies of conceptual fuselage section and bulkhead for comparative weight analysis and optimization. Alternate concepts are also considered for systems study in an attempt to improve the present design farther. Only local idealized fuselage section is considered in this paper, with a limited set of critical design loads. The objective is to minimize the local structural weight by 10-20% with stitched composite construction combined with novel structural configuration, compared to the sandwich and multi-bubble concepts that were studied previously. At the vehicle level, aerodynamic and structural systems study for the 100, 200, 300, and 400-passenger versions were considered

in Refs. 19-23, in order to estimate the full vehicle structural weight at all critical load conditions. For a recent multi-bubble HWB configuration study, see Ref. 24.

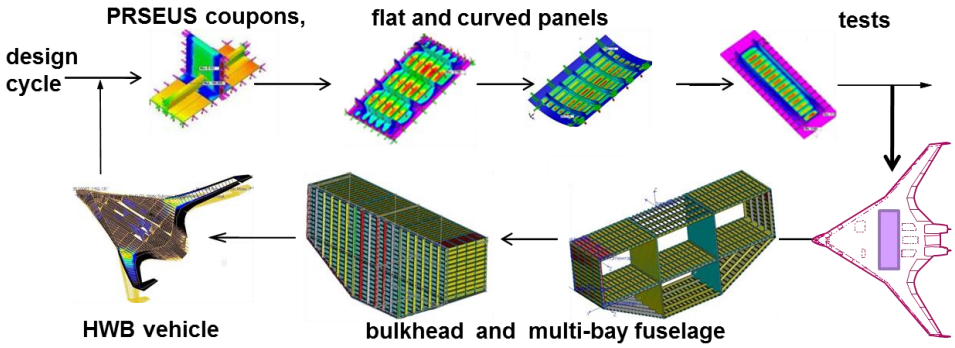

Figure 2. PRSEUS concept development cycle for analysis, design and testing.

II. Classical Stiffened Plate Analysis

Since the Finite Element (FE) model development of the PRSEUS concept requires many levels of simplification and idealization for extension from the coupon level to the fuselage level[18], an analytical model is developed at the panel level for rapid parametric study and sizing. This would also enable one to evaluate the effects of skin thickness, frame and rod-stringer spacing and section geometry on the panel deflection due to a pressure load and for buckling analysis due to in-plane compression load. Classical plate theory[25-26] and equivalent orthotropic stiffened plate equations[27-29] were applied to simplify the PRSEUS model analysis for a rectangular plate. These simple spread-sheet based analytical results are also used for sanity check of the high fidelity FE analysis of panels, fuselage section and bulkhead. SolidWorks[30] was used for rapidly building detailed FE models of the vehicle fuselage sections for structural analysis and design. A large number of design options were considered such as the orthotropic skin thickness, frame and rod-stringer spacing, for obtaining stress and strain distributions, deformation pattern and for identifying critical areas. For each configuration, structural weight was computed and compared.

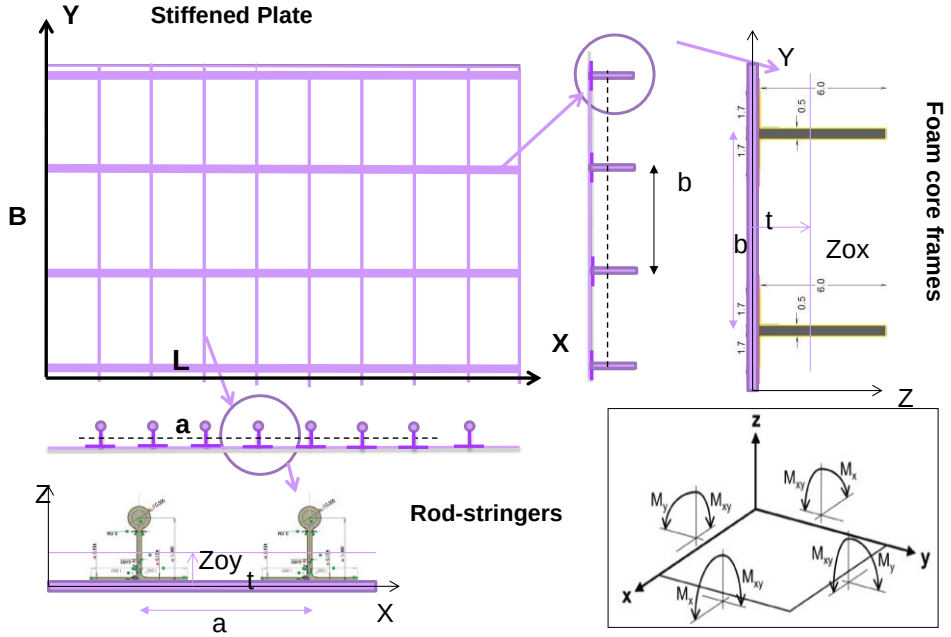

Figure 3. Frame and pultruded rod-stringer stiffened orthotropic plate configuration.

Stiffened Plate Bending Analysis: Consider the biaxially stiffened plate shown in Fig. 3. For an isotropic thin rectangular plate of uniform thickness *t*, length *L* and width B, the maximum deflection can be expressed as in Eq. 1 which is a function of the pressure load q, plate bending stiffness *D* and the factor *k* that is calculated from analytical

solution for this boundary condition. The factor k is presented in tabular form [25], as a function of the ratio B/L (B>L). For example, for a square plate with built-in edges, *k=0.00126* for *B/L=1* (Table 1). For a simply supported isotropic square plate, k = 0.00406.

(1) $w_{max} = k.qL^4/D$ where $D = Et^3/12(1-\nu^2)$

Let us assume that the uniform plate-theory assumptions are also applicable to this equivalent stiffened plate. From ideal orthotropic plate theory [25], for a simply supported stiffened rectangular plate, the closed form solution for deflection w given by Eq. (2).

$$(2)\quad w(x,y) = \frac{16q_o}{\pi^6}\sum_{m=1,3,5}\sum_{n=1,3,5}\frac{\sin(m\pi x/L)\sin(n\pi y/B)}{mn\left(\frac{m^4}{L^4}D_x+\frac{2m^2n^2}{L^2B^2}H+\frac{n^4}{B^4}D_y\right)}$$

The running stifnesses D_x , D_y and H can be approximately defined[25-29] by Eqs. (3-5).

$$(3)\quad D_x = \frac{E_x t^3}{12(1-\upsilon_x\upsilon_y)}+\frac{E_x t Z_{ox}^{\ 2}}{12(1-\upsilon_x\upsilon_y)}+\frac{E'_x I_x}{b}$$

$$(4)\quad D_y = \frac{E_y t^3}{12(1-\upsilon_x\upsilon_y)}+\frac{E_y t Z_{oy}^{\ 2}}{12(1-\upsilon_x\upsilon_y)}+\frac{E'_y I_y}{a}$$

$$(5)\quad H = \sqrt{D_x D_y}$$

The terms in Eq.(3-4) are explained in Figure 3. The equivalent plate bending stiffnesses D_x, D_y resists bending moment M_x, M_y about the *x*-and *y*- axes, respectively. The attached longitudinal stiffening frames, each with area A_{sx} and individual bending stiffness E'_xI_x move up the cross-sectional-area center by Z_{ox} from the plate neutral (mid) plane, thereby increasing the total area and the bending stiffness. The symbol E'_x is used to differentiate the stiffener modulus from the plate modulus E_x. Similarly, the transverse stringers or rod-stiffeners, each with area A_{sy} and bending stiffness E'_yI_y, increase the bending stiffness D_y by moving up the transverse-section-area center by Z_{oy} from the plate neutral plane.

For the stitched composite orthotropic skin, the following material properties were used[8-9], namely $E_x = 9.75\times10^6$ psi, $E_y = 4.86\times10^6$ psi, $\nu_x = 0.39$, and $\nu_y = 0.2$. A stitched composite frame with a 0.1inch skin wrapped around a 6 inch high, 0.5 inch thick foam core and a 4-in. wide flange and a 0.1 inch thick base cover strap provide a cross-sectional area of approximately 2 in.^{2}, without considering the foam core, that is mostly for shape stabilization. The frame dimensions are schematically shown in Figure 4(a). The frame flange is stitched to the base skin and are spaced at b=20 in. interval, and with a 0.1 in. skin thickness, the skin area between the frames is approximately 2 in^2. Together, the frame and the skin segment between adjacent frames have running bending stiffness D_x of approximately *5.8×10^6 lb-in*. By using a 0.2 inch thick frame cap (Fig. 4b), D_x increases to *6.3x10^6 lb-in*. This would reduce the stresses, which are highest in the frame cap. For the first rod-stringer shown in Fig.4c, with base to rod-center height of 1.4 in., D_y = *0.75x10^6 lb-in.* including a *2 in.* cover-strap and base skin between the rod-stringers spaced at *6* inch apart. For the rod-stringer in Fig.4d, with base to rod-center height of *1.65 in.*, D_y=*1.08x10^6 lb-in*. The rod-stringer in Fig.4e, with *0.208 in*. flange thickness, and

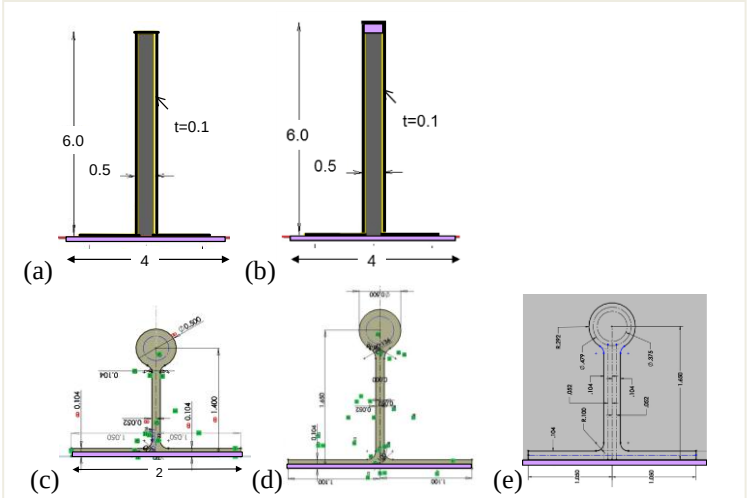

Figure 4. Frame and rod-stringer configurations.

base to rod-center height of *1.65 in.*, $D_y=1.45x10^6$ *lb-in*. Next, these frame-stiffened plate stiffness estimates were applied to the classical isotropic plate bending equations. The D_x, D_y and H that were computed for this frame-stiffened panel are now applied to a classical plate bending equation subject to a normal, uniform distributed pressure load of *q* psi with simple-supported and clamped edge conditions[25-26].

Simply Supported Plate: Using Eq. (2) to an anisotropic rectangular plate with $q_o=18.4$ *psi*, $L=120$ *in.*, $B=90$ *in.*, $D_x = 5.77\times10^6$ *lb-in* and $D_y = 0.75\times10^6$ *lb-in.*, the maximum deflection is 4.5 in. Here, stiffer frames (D_x) running along the longer side L, as shown in Fig. 3. If the frames are running along the shorter side *B*, and the rod-stringers are running along the longer side *L*, then the deflection can be obtained by simply interchange D_x with D_y in Eq.(2). The deflection at mid-point is now reduced to 2.1 inches.

If we apply Eq. (2) to a simply supported isotropic square plate ($L=B$, $D_x=D_y=D$) the maximum deflection is can be simply written as in Eq. (1), $w_{max}=kqL^4/D$ with $k = 0.00406$. If one takes just the first term ($m=1$, $n=1$) in Eq. (2), i.e. $w_{max}= (16/\pi^6)/ (D_x/L^4+2H/L^2B^2+D_y/B^4)$, then for a square plate $k=4/\pi^6=0.00416$. With $q=18.4$ psi, $D_x = 5.8\times10^6$ *lb-in* and $D_y = 0.75\times10^6$ *lb-in*, application of the exact Eq. (2) gives w_{max}=3.23 inches, for a 104-in. square panel.

For an orthotropic plate, one may modify Eq. (1) to $w_{max}= kqL^4/\sqrt{(DxDy)}$ by replacing *D* with $\sqrt{(D_xD_y)}$, with applicable k value. For example, with this approximation, for the same 104-in. square panel, the maximum deflection w_{max}=3.52 in., about *9%* higher than that from Eq. (2). This simple approximation, $w=kqL^4/\sqrt{D_xD_y}$ may provide reasonable results for maximum deflection, for appropriate k value from Table 1[25, 26].

Table 1: Clamped Isotropic Plate max deflection with uniform pressure q:				20	6	0.104	1.65	0.104	0.479
Uniformly loaded Clamped isotropic stiffened plate: Table 35, p 202, nu 0.3 figure 91 p 197 Timoshenko									
CASE NO	**max deflection equation**	**length L (L< B)**	**width B**	**stiffness Dx, Dy or sq**	**load q (psi)**	**k**	**max deflection wmax=kqL^4/D**		**shell skin t**
1	wmax=kqL^4/Dx, L=B	120	120	5,805,106	18.4	0.00126	0.83		0.104
2	wmax=kqB^4/Dy, L=B	90	90	1,087,872	18.4	0.00126	1.40		0.104
3	wmax=k.q.(L^4)/sqrt(Dx*Dy), L=B	104	104	2,513,008	18.4	0.00126	1.08		0.104
4	wmax=k.q.(L^4)/sqrt(Dx.Dy), B/L=1.3	90	117	2,513,008	18.4	0.00191	0.92		0.104
5	wmax=k.q.(L^4)/sqrt(Dx.Dy), B/L=1.33	90	120	2,513,008	18.4	0.00196	0.94		0.104
6	wmax=k.q.(L^4)/sqrt(Dx.Dy), B/L=1.5	80	120	2,513,008	18.4	0.00220	0.66		0.104
7	wmax=kqL^4/Dx, B=2L B/L=2	60	120	5,805,106	18.4	0.00254	0.10		0.104
8	wmax=kqL^4/Dy, B=2L B/L=2	90	180	1,087,872	18.4	0.00254	2.82		0.104
9	wmax=k.q.(L^4)/sqrt(Dx.Dy), B=2L	90	180	2,513,008	18.4	0.00254	1.22		0.104
10	wmax=k.q.(L^4)/sqrt(Dx.Dy), B = 1.55 L	90	140	2,513,008	18.4	0.00225	1.08		0.104
11	max=4*k.q/[Dx/L^4 +2H/(L^2.B^2) + Dy/B^4]	80	120	5,805,106	18.4	0.00220	0.80	Dx -> L (L<B)	0.104
	B/L=1.5 (L<B) switch Dx and Dy	80	120	Dx and Dy					
12	max=4*k.q/[Dy/L^4 +2H/(L^2.B^2) + Dx/B^4]	80	120	1,087,872	18.4	0.00220	1.48	Dy -> L (L<B)	0.104

Table 1: Clamped isotropic plate maximum deflection with single wrap rod-stringer at 6 inch spacing and double wrap frames at 20 inch spacing with uniform normal pressure of 18.4 psi.

CASE NO	**fsp 24 rsp 8 t = 0.104**	**fsp 24 rsp 8 t=0.052**	**fsp 24 rsp 6 t = 0.104**	**fsp 24 rsp 6 t=0.052**	**fsp 20 rsp 6 t = 0.104**	**fsp 20 rsp 6 t=0.052**	**fsp 20 rsp8 t = 0.104**	**fsp 20 rsp 8 t=0.052**	**max deflection equation**
1	0.97	1.07	0.97	1.07	0.83	0.92	0.83	0.92	wmax=kqL^4/Dx, L=B
2	1.77	1.89	1.40	1.47	1.40	1.47	1.77	1.89	wmax=kqB^4/Dy, L=B
3	1.31	1.42	1.16	1.26	1.08	1.16	1.21	1.32	wmax=k.q.(L^4)/sqrt(Dx*Dy), L=B
4	1.11	1.21	0.99	1.07	0.92	0.99	1.03	1.12	wmax=k.q.(L^4)/sqrt(Dx.Dy), B/L=1.3
5	1.14	1.24	1.02	1.10	0.94	1.02	1.06	1.15	wmax=k.q.(L^4)/sqrt(Dx.Dy), B/L=1.33
6	0.80	0.87	0.71	0.77	0.66	0.71	0.74	0.81	wmax=k.q.(L^4)/sqrt(Dx.Dy), B/L=1.5
7	0.12	0.14	0.12	0.14	0.10	0.12	0.10	0.12	wmax=kqL^4/Dx, B=2L B/L=2
8	3.56	3.81	2.82	2.96	2.82	2.96	3.56	3.81	wmax=kqL^4/Dy, B=2L B/L=2
9	1.48	1.61	1.32	1.42	1.22	1.32	1.37	1.50	wmax=k.q.(L^4)/sqrt(Dx.Dy), B=2L
10	1.31	1.43	1.17	1.26	1.08	1.17	1.21	1.33	wmax=k.q.(L^4)/sqrt(Dx.Dy), B = 1.55 L
11	0.95	1.05	0.91	1.01	0.80	0.89	0.83	0.92	wmax=4*k.q/[Dx/L^4 +2H/(L^2.B^2) + Dy/B^4]
	B/L=1.5 (L<B) switch Dx and Dy								B/L=1.5 (L<B) switch Dx and Dy
12	1.80	1.96	1.60	1.73	1.48	1.61	1.66	1.81	wmax=4*k.q/[Dy/L^4 +2H/(L^2.B^2) + Dx/B^4]

Table 2. Parametric maximum deflections for the 12 cases in Table 1 for a combinatorial set of frame spacing (fsp=20 or 24 in.), rod-stiffener spacing (rsp=6 or 8 in.) and skin thickness (t=0.052 or 0.104 in.).

Clamped Edge Plate: One can apply this approximation to the Eq. (1) for a clamped edge plates (Ref. 25, Figure 91, pp.197, and Table 35, pp. 202). Table 1 shows the maximum deflection of typical rectangular clamped panels with $D_x=5.8x10^6$ *lb-in.*, $D_y=1.08x10^6$ *lb-in.* (Frame in Fig.4a, rod-stringer in Fig. 4d, respectively), and 18.4 psi pressure

load. The equivalent plate bending stiffness D_x or D_y were computed from Eqs. (3-4) from classical plate theory with 20 inch frame spacing, 6 inch rod-stringer spacing, 0.104 inch skin and frame-wrap thickness.

The column at left shows the equation used for each of the 12 cases. Case 1 is for a frame stiffened (D_x) square plate in both directions x and y. Case 2 is for rod-stringer stiffened (D_y) square plate in both directions x and y. In the cases 3 to 6, 9 and 10, stiffness D is replaced by $\sqrt{(D_x.D_y)}$ *as* an equivalent orthotropic approximation, as discussed before. In case 3, for a *104 in*. square plate, the maximum deflection is approximately *1.08* in. with $q=18.4$ psi. In case 10, a *90x140* stiffened plate (lower bay side-cargo panels) this approximation yields a maximum deflection of 1.08 inches. These approximations yield a median deflection value that cannot distinguish between running direction of frames and rod-stringers in rectangular panels. Hence, in case 11, D/L^4 in Eq. (1) is replaced by $0.25[D_x/L^4+2H/(L^2B^2)+D_y/B^4]$ with k factors for the specific B/L ratio (L<B) from Ref. 26, for a better orthotropic approximation. This equation represents stiffer frames (D_x) running along shorter direction L and the maximum deflection is 0.8 inches for an *80x120* panel. In case 12, D/L^4 is replaced by $0.25[D_y/L^4+2H/(L^2B^2)+D_x/B^4]$, (Interchange D_x with D_y) which represents stiffer frames (D_x) running along the longer direction B. In this case the maximum deflection is 1.48 inches. This characteristic is similar to that observed from the exact Eq. (2) for the simply supported orthotropic rectangular plate case. Of course, for square orthotropic plate, both equations yield same deflection.

Table 2 (continuation of Table 1) shows maximum deflections for each of the 12 cases, which are computed for eight combinatorial design scenario of frame spacing of 20 and 24 inches, rod-stringer spacing of 6 and 8 inches and skin thicknesses of 0.052 and 0.104 inches. These spread sheet based calculations can be used for panel sizing, weight and configuration optimization as well as for sanity check of numerical finite element results.

Ideal Beam-Column Buckling analysis: Consider an ideal straight beam-column to represent a flat cabin roof panel segment, with axial in-plane compression load P, and distributed running load q due to the normal cabin pressure. Let EI be the beam bending stiffness over the span-length L. From the beam-column theory, the maximum deflection, bending moment, and bending stresses at mid-span are given by Eqs. (6-8).

(6) $w_{max} = (qL^4/384EI)\eta(\mu)$, where $\eta(\mu)=12(2.\sec(\mu) -2 - \mu^2)/(5\mu^4)$

(7) $M_{max} = (qL^2/8) + P_c.w_{max}$, where $\mu = \frac{L}{2}\sqrt{\frac{P_c}{EI}}$

(8) $\sigma = M_{max}\, z/I \pm P_c/A$

The critical bucking load P_{cr} for a simply supported straight beam without initial deformation or eccentric loading is given by $P_{cr} = \pi^2 EI/L^2$. Then $\mu = (\pi/2)\sqrt{(P_c/P_{cr})}$, and thus these equations are valid for $P_c < P_{cr}$, or $\mu < \pi/2$. Based on the beam-column equations, the stiffener frame dimensions can be sized to provide adequate section area and bending stifnesses to prevent buckling. In these beam bending calculations, in order to represent a stiffened panel, the total bending stiffness EI in beam-column equation is replaced with $D_x b$, and the total spanwise running load q is multiplied by b, where b is the frame spacing. Applying the simply supported beam-column Eqs. (6-8) with $L=120$ in., $b=20$ *in*. $D_x=5.8x10^6$ *lb-in.* (Frame in Fig.4a), and a *9.2 lb/in*. normal running load, the maximum linear deflection is 4.28 in. and the maximum bending stress on the frame top is *6,000 psi* without compression load. The critical beam-buckling compression load is *3960 lb/in*., assuming that the frame and the plate segment bend like a beam. With a compression load P_c=1000 lb/in., $P_c/P_{cr}=0.25$ and the maximum nonlinear deflection is 5.72 in. The maximum bending plus axial stress is 49,000 psi including non-linear bending effect due to the 1000-lb compression load. Hence, for a simply supported ideal frame-stiffened beam-column, the buckling strength needs to be increased significantly.

In the real situation, the PRSEUS panel will be cross- stiffened and all edges will be close to the clamped condition. The beam deflection for the clamped case can be computed by applying equal end-moments M_o, which would reduce the end-slopes to zero. This moment and the corresponding maximum deflections are given by[26] Eqs. (9-10).

(9) $M_o = -(q.L^2/12).\ \mu.\chi(\mu)/\tan(\mu)$, *where* $\chi(\mu)=3(\tan(\mu)-\mu)/\mu^3$

(10) $w_{max} = (MoL^2/8.EI).2(1-\cos(\mu))/\mu^2\cos(\mu)$

For the clamped end condition, the linear buckling load $P_{cr}=4.\pi^2EI/L^2$ *or 15,000 lb./in.* in-plane compression running load. The end moment M_o is calculated to be *230,000 lb-in*, and the corresponding maximum bending stress at the

frame-top is approximately *78,000 psi* at beam ends. The maximum non-linear deflection at mid-span is then *4.8 inches*. In order to reduce the deflection and alleviate this high local stress, the panel skin and frame ends need to be reinforced significantly.

Panel Buckling Analysis: Consider the simply supported stiffened plate in Fig.3 under normal loading q and in-plane compressive running load N_x, then the solution for deformation can be expressed as a modified form of Eq.(2)

$$(11)\quad w(x,y)=\frac{16q_o}{\pi^6}\sum_{m=1,3,5}\sum_{n=1,3,5}\frac{\sin(m\pi x/L)\sin(n\pi y/B)}{mn(\frac{m^4}{L^4}D_x+\frac{2m^2n^2}{L^2B^2}H+\frac{n^4}{B^4}D_y-\frac{N_x m^2}{\pi^2L^2})}$$

The value of N_x that renders the denominator of Eq. (11) to zero will provide the in-plane buckling load. Thus for m=1, n=1, in-plane compressive running load $N_{xcr} = \pi^2L^2[D_x/L^4 + 2*H/(L^2.B^2) + D_y/B^4]$. For the orthotropic equivalent plate with *L=120 in., B=90 in.*, $D_x = 5.80\times10^6$ *lb-in* and $D_y = 1.08\times10^6$ *lb-in*, the critical in-plane running load N_{xcr} is *12,000 lb/in.* For an isotropic square plate, the critical minimum buckling is given by $N_{xcr} = 4\pi^2D/L^2$. For a *104x104 in*. square simply supported plate with *D* replaced by $\sqrt{(D_xD_y)}$, $N_{xcr} = 9100$ *lb/in.*

III. Fuselage Section Analysis.

Design conditions: The following critical design load conditions were studied for the fuselage and bulkhead.

1. *18.4-psi* internal static over-pressure at ground level (i.e., 2P case).
2. *2.5-g* climb condition with an internal cabin pressure of *9.3 psi* (i.e., 1P-2.5g case).
3. Panel in-plane buckling load of *5000 lb/in*. with *9.3 psi* normal cabin pressure.

The maximum aerodynamic load for the *1P-2.5g* case also produces a maximum compression load on the fuselage top panels and a maximum tensile load on the fuselage bottom panels. This bending load is idealized as approximately 5000-lb/in. running compression and tension load along the top and bottom panels, respectively. This in-plane ultimate design load was derived from full-vehicle FEM analysis results[14-16] and includes all safety margins.

Material Properties: For the orthotropic stitched PRSEUS panel, the elastic modulus in the *x* and *y* directions are $E_x = 9.75\times10^6$ *psi*, $E_y = 4.86\times10^6$ *psi*, $\upsilon_x = 0.39$, $\upsilon_y = 0.2$, respectively. The average mass density is 0.057 lb/in^3. For the foam core, *E = 21000 psi, G = 7950 psi*, and the mass density is *0.00361 lb/in*^{3}. The web and the flange of the pultruded rod-stringer have the same property as the stitched composite material. The pultruded rod has an elastic modulus of $E' = 1.9\times10^7$ psi and $\upsilon = 0.29$. This property is used when the built-up rod-stringer is modeled as a beam. In some of the previous panel analysis[18] the web was modeled as shell and the top bulb was modeled as a beam. The stronger *x*-direction of the orthotropic skin and frame-wrap are always along the frame running direction.

Failure Criteria: In the linear analysis, the maximum allowable principal strain is *0.007* for the orthotropic skin and frame wraps. For the orthotropic skin and built-up pultruded rod-stringer average yield stress of F_{ty} = *46500* psi is used for a conservative safety factor calculation. For solid models of the foam-core, yield stress F_y = 440 psi. The allowable failure stresses of the orthotropic shell are F_{tx} = *105100* psi, F_{ty} = *46500* psi, in tension, and F_{cx} = *79200* psi and F_{cy} = *37900* psi in compression, respectively. The maximum allowable

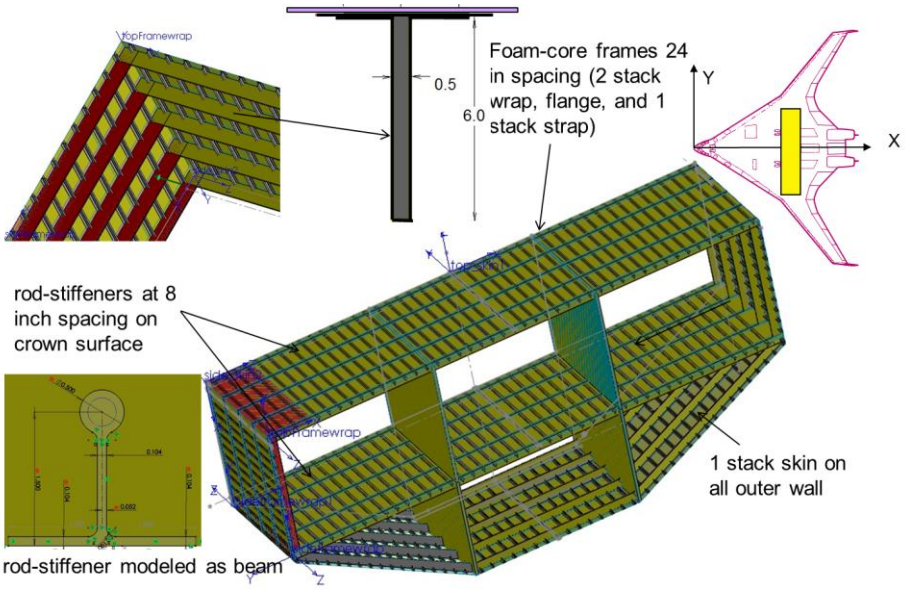

Figure 5. Multibay model with 5 frames at 20 inch spacing, and rod-stringers at 8 in.

shear stress is *29900* psi. When the rod stringers were modeled as beams, the maximum combined bending and axial stresses were used to check for beam failure. The directional stresses and principal strain distributions along with yield stress based factor of safety were plotted to identify local high stress and strain failure areas.

Multibay Fuselage Section: For a detailed description of the Multibay development, fabrication and combined loads test plan and progress, see Refs. 11-16. Figure 5 shows a multi-bay concept models along with the frame and rod-stringer dimensions. This model is substantially simplified, from those described in refs. 11-16, in order to facilitate conceptual study and what-if type analysis. This 3 bay section has a spanwise width of 360 inches, with 90 inch high passenger bay, 72 in. high central cargo bay. This fuselage section has five foam-core frames at 20 in. spacing. Each frame is built-up with 6 in. high, 0.5 in thick foam-core, that are wrapped with 0.104 in. thick (2 stack) composite skin and flanges. The flanges are stitched to the base skin and frame cover straps. The rod-stringers are spaced 8 in. apart on upper and lower surface of each bay, side walls, lower left and right cargo bay and passenger floors. Each rod-stringer is built-up with stitched composite flange, web wrapped around a pultruded carbon rod shown in Fig 4d. The flange is stitched to the base skin and a stringer cover strap[16]. In this multi-bay concept analysis, the built-up rod-stringers are modeled by beam elements with same cross-section as the built-up rod-stringer and cover strap. The base skin and frame wraps are modeled by shell elements. The foam core is modeled by solid elements. The two mid-cabin sandwich walls are modeled with 2 in. thick foam core and 0.052 in. stitched composite skin without cutouts.

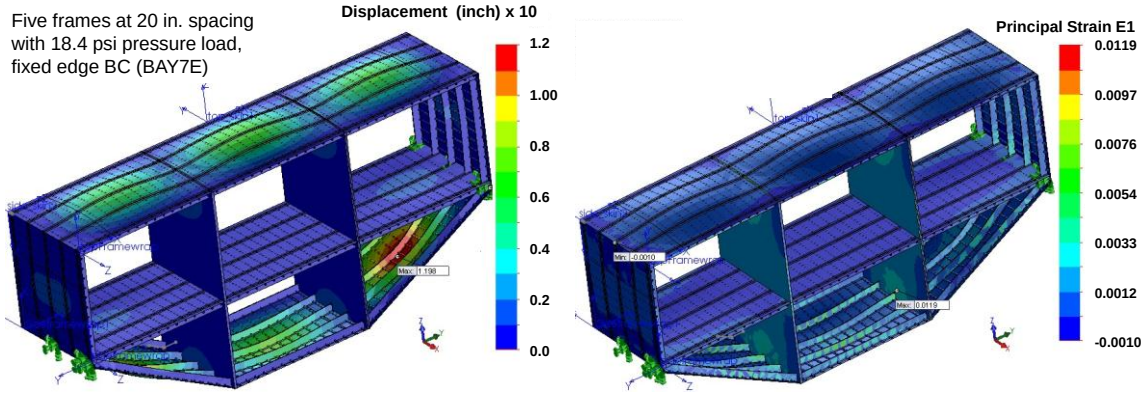

Figure 6. Multibay displacements (magnified by x10) and principal strain (Five frames at 20 inch spacing, improved rod-stringer at 8 in. spacing, without bulkhead) under internal cabin pressure of 18.4 psi and passenger-floor pressure of 1 psi.

Figure 6 shows the corresponding displacements (magnified by x10) and principal strain under 18.4 internal cabin pressure on all outer walls and 1 psi pressure on passenger floors. Since the bulkhead was not modeled, an all outer-edge-fixed boundary condition was applied. The maximum deflection on the right and left side slanted cargo compartment walls is 1.2 in. Note that the cargo bays are approximated as flat panels, although in actual vehicle these keel panels conform to the aerodynamic shape. The directional stresses and strains on the skin are generally within the allowable limits, except at edge-restraints, cabin-wall-skin junctions, corner junctions and foam-core frame areas. The maximum principal nodal strains are of the order 0.012, at inter-cabin-junctions and unreinforced cabin-corners. In order to reduce large local stresses, these junctions need to be modeled more realistically with doubler and corner braces. These corner junction areas require diagonal braces and additional reinforcements. Additional design refinements are required in these critical areas. The maximum bending and axial stresses on the rod-stiffeners, which were modeled as beam elements are generally within allowable limits, but may exceed locally at the lower cargo bay due to large bending and edge constraints. The stress safety factors are locally 0.5 in this area on the rod-stiffeners but are well above 1 elsewhere. These high stresses can be reduced by adding corner braces, rod-stiffeners with a higher bending stiffness and frames with thicker frame-caps in these areas along with at least 0.1 in. skin due to impact damage concerns. The maximum deflection values from the FE analysis are close to the empirical average values, shown in Tables 1 and 2 (cases 6 and 10) and generally consistent with the analytical deflection values of similar size stiffened plates. However, there are still some unresolved issues about the analytical solution of orthotropic clamped plates, including buckling analysis, which will be addressed in future. An isolated test bulkhead analysis is presented next.

IV. Bulkhead Analysis

Fig. 7(a) shows the displacement of an isolated bulkhead configuration with 20 horizontal rods at 8 inches spacing, 19 vertical frames at 20 inches spacing, two stack skin and two stack frame-wrap. Under the 18.4 psi pressure, maximum deflections are of the order 1.13 inches on the upper bulkhead left and right bay segments. The principal strain is generally under 0.007 inch/inch. Local combined maximum axial and bending stresses on the horizontal rod-stringers that were modeled as beam are under 76000 psi. Except for the local stress at the bulkhead-wall joints, due to end-fixity conditions, the majority of resultant stresses are under 70,000 psi. These high stress and deflection can be reduced significantly, by reinforcing the rod-stringers with two-stack wrap as discussed earlier. This is shown in Figure 7(b). The maximum deflection is now reduced to about one inch. The outer bay width for this configuration is reduced by 6 in. on each side. The local maximum beam bending stresses are now under 80,000 psi. The local maximum principal strains are now under 0.007 in/in. The deflections are close to the analytical values presented in Tables 1 and 2 (cases 5 and 11). However the total weight increases slightly to 878 lb. (2.59 lb/sq. feet of surface area), as shown in Table 3.

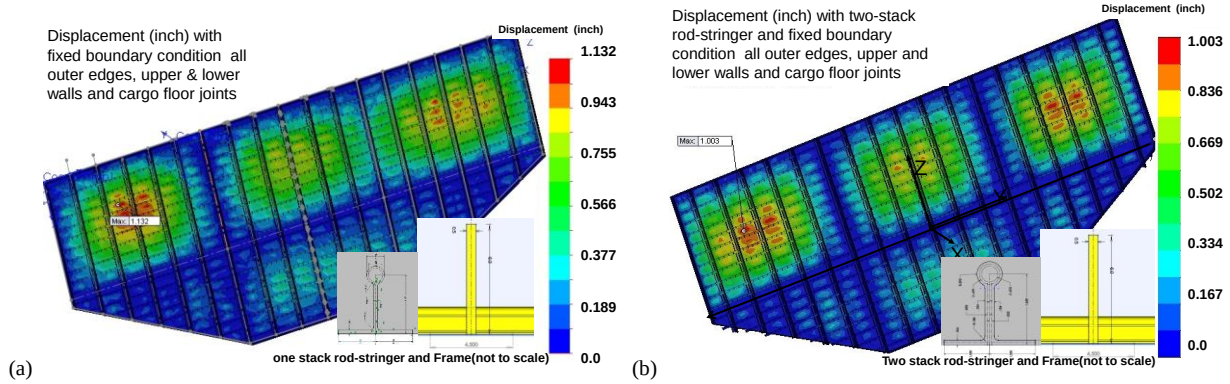

Figure 7. Bulkhead displacements under an 18.4 psi normal pressure load with fixed end boundary conditions: (a) one stack rod-stringer (Fig. 4d) and (b) two stack rod-stringer (Fig. 4e) with 1.65 inch base to center height.

new two stack 1.65b2c rod_dim										
weight calculation Bulkhead2T (2 stack skin, 2 stack wrap, strap, 8 inch rod spacing, 24 in frame spacing) Study 2										
BULKHEAD2b	width	length	area	thickness	vol.	density	weight/each		weights	group
study 2 (SW13)	inch	in	in^2	in	in^3	lb/in^3	lbs	X no items		weight
skin group										292
top panels	90	348	31320	0.104	3257.3	0.057	185.7	1	185.7	
lower mid bay panel	72	120	8640	0.104	898.6	0.057	51.2	1	51.2	
triangular panels 2	72	114.0	4680	0.104	486.7	0.057	27.7	2	55.5	
2 stack	rod area	web area	flange are	area	length	density		no of rods		
Hor rod-stringer group	in^2	in^2	in^2	in^2	in^3	lb/in^3	lbs	x no		305
rod_stringer 1.65 in b2C										
2.1 in base @ 8 in	0.267865	0.260832	0.3276	0.856297	360	0.057	17.6	17.33333	304.6	
Ver Frame group	width	length	area	thickness	vol	110wf cSW		x no		281
frame core at 24 inch	6	162	972	0.5	486.0	0.0036	1.7	13.1	23.0	
frame wrap+flanges	16.5	162	2673	0.104	278.0	0.057	15.8	13.1	208.0	
frame base strap	4	162	648	0.104	67.4	0.057	3.8	13.1	50.4	
Total Weight (lbs)				Total weight (lbs)					878	878
projected Area			48852		339.25	sq ft		lb/ft^2	2.59	

Table 3. Component weight breakdown of a test bulkhead FE model with vertical frames.

V. Integrated Multibay and Bulkhead

The Mixed model of integrated multi-bay with bulkhead model, shown in Fig. 8, was studied for two purposes; 1) Simplify the model to determine an equivalent plate to represent the bulkhead and cargo-bay for 2P load; and 2) Capture the critical are area behavior for asymmetric bending-torsion loads. The upper crown panels and side 1 bulkheads are modeled with foam-core frames and rod stringers. The bulkhead side 2 is modeled with 1.5 inch thick equivalent flat plate. The bulkhead side 2 is hidden to show the interior details. Bulkhead side 2 upper and lower bays and cargo bays were also modeled with semi-equivalent plate of 1.5 inch thickness. The equivalent thicknesses

were selected to provide same order of deflection on both bulkhead side 1 (stiffened thin shell) and side 2 (uniform shell). Figure 9 shows the corresponding displacements and principal strain with 18.4 psi internal cabin pressure. Although the equivalent plates cannot be used for buckling analysis, they are necessary for scaled system study, comparison with theory, and for building simplified full vehicle model for flight load analysis. This model is presently being developed. Integrated PRSEUS fuselage and bulkhead models will also be developed farther for in-plane load and buckling analysis.

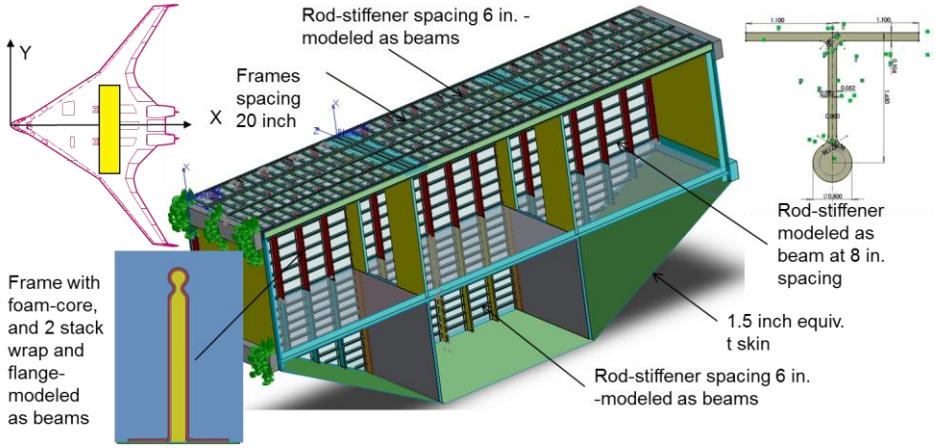

Figure 8. Integrated multi-bay fuselage section and pressure bulkhead configuration.

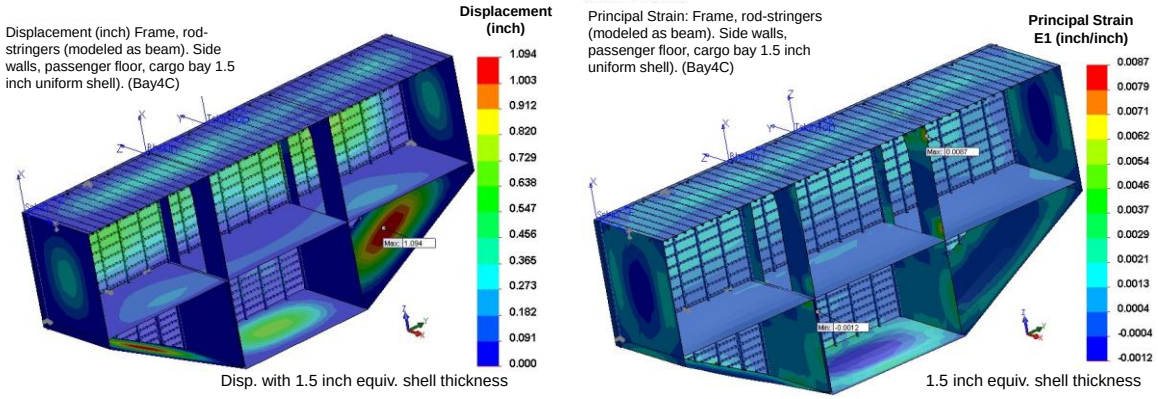

Figure 9. Integrated multi-bay fuselage section displacement and principal strain with 18.4 psi cabin pressure.

VI. Summary of FEM Weight Analysis

The first and second-generation 800 passenger HWB concepts were developed at Boeing Phantom Works through NASA contract and NASA in-house research[1-5]. In Ref. 5, four structural concepts were studied, namely, Vaulted Ribbed Shell (VLRS), Flat Ribbed Shell (FRS); Vaulted shell with Light Honeycomb Core (VLHC) and Heavy Honeycomb Core (VHHC); and Flat sandwich shell with Light and Heavy Honeycomb Core (FLHC & FHHC). A multi-bubble section concept was analyzed in Ref. 6 and a relative comparison of component non-optimal weight breakdown per unit surface area is shown in the first bar chart in Figure 10. Conventional two floor cylindrical and A380 type elliptic section and stress balanced multi-bubble fuselage sections with frame and longiron stiffened aluminum skin of 3 mm (0.118 inch) shell thickness were also analyzed for comparison.

The weight analysis summary of the Multibay (without pressure bulkhead) is shown in the 3rd bar charts in Figure 10. The weight analysis includes three design scenarios: 1) 2 stack skin and rod-spacing of 8 in.; 2) 2 stack skin and rod-spacing of 6 in.; and 3) 1 stack skin and rod-spacing of 8 inches. Passenger floor has 1 stack skin and rod-spacing of 8 in. The frames are at *20 inch* spacing for all 3 cases. The Multibay configuration weight with 2 stack skin and 2 stack frame wrap appears be a safe-design for this internal pressure load case. The weight can be reduced by using a single stack skin configuration, but the impact damage can be a serious concern. The estimated weight of the multi-bay with 1 stack skin and two stack frame wrap is approximately *1800 lb.* (about *1.92 lb/sq. ft* of surface

area) for one stack skin and two stack frame wrap, 8 inch rod-spacing). The maximum deflections are of the order *1.37 inches* at outer skin surface of the cargo area (Figure 6). The maximum stresses are of the order *69,000 psi* on the skin at the corner junction. The maximum strains are of the order *0.007 in./in.*, but local strains are higher at corner junctions. In the 4th bar chart, estimated specific weights of three bulkhead configurations are presented from preliminary analysis of three configurations: 1) 2 stack skin, 2 stack rods at 8 in spacing (Fig.7b); 2) 2 stack skin, 1 stack rods at 8 in spacing (Fig.7a); and 3) 1 stack skin, 2 stack rods at 8 in spacing. In all case the vertical frames are at 24 inch spacing. In the first case, the bulkhead weight is 878 lb (2.6 lb/sq. ft. surface area) without considering edge reinforcements and attachment fittings. The maximum defection is about 1 inch. The stresses and strains are generally within the allowable limits. Although the weights can be reduced in the 2nd and 3rd configuration, the deflection and stresses can be significantly higher.

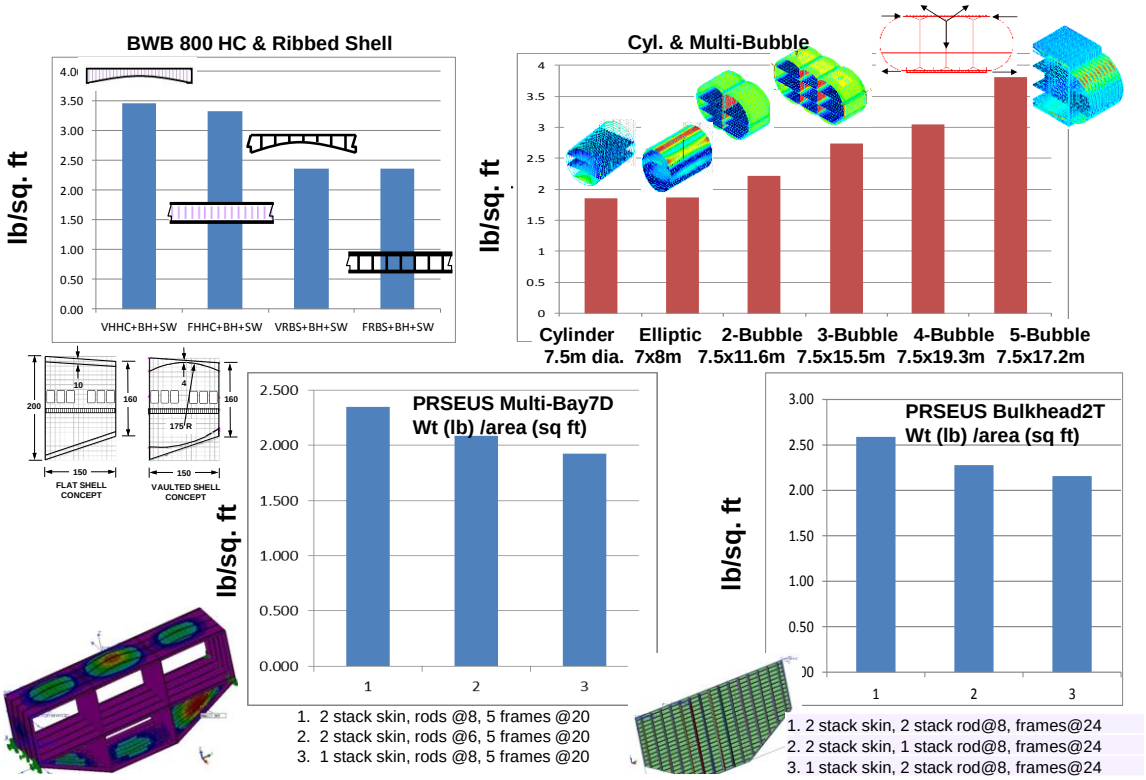

Figure 10. Summary of relative non-optimal finite element model concept weight per unit surface area.

VII. Conclusions

This finite element analysis and trade studies of a hybrid-wing-body fuselage section indicate that advanced, stitched, composite stiffened plates with rod-stringers and foam-core frames are better than the vaulted double-skin-shell or multi-bubble stiffened-shell concepts. A combination of skin-thicknesses, rod-stringer spacing and frame spacing were considered for the weight reduction trade study. The finite-element-model based specific weights of an ideal three-bay section and bulkhead model are estimated to be 2.0 lb./sq. ft. and 2.6 lb./sq. ft., respectively, depending on the configuration. These specific weight values are comparable to that of the cylindrical fuselage, but are lower than multi-bubble concepts, for the 18.4 psi pressure load condition. Although, 0.052 inch (1 stack) outer skin is preferable from a minimum weight perspective, additional load conditions and buckling studies indicate that 0.104 inch (2 stacks) skin will provide better safety margins and impact damage resistance. Since the sandwich frames take most of the bending load, two stacks of frame-wraps and frame caps are necessary. The combined maximum local bending and axial stresses in the rod-stringers also appear to be high at end-joint areas. With continuing development and testing, this stitched composite technology could make the current hybrid-wing-body concept both structurally feasible and aerodynamically efficient. But, the adverse effect of pillowing on the outer-surface aerodynamic flow should be considered. Systems analysis of the stitched composite bi-axially stiffened shell concept demonstrated that the hybrid-wing-body class of vehicles can be structurally as efficient as

the conventional cylindrical skin-stringer-frame construction. However, alternate concepts should also be considered to improve the present design farther.

VIII. Acknowledgments

This research was done under the NASA Environmentally Responsible Aviation (ERA) and Subsonic Fixed Wing (SFW) projects in collaboration with both the Boeing Company, Huntington Beach, CA, and the Air Force Research Laboratory (AFRL). The author wishes to thank Dr. Fayette Collier, Project Manager, ERA Project; Anthony Washburn, Project Engineer; Pamela Davis, Assoc. Project Manager, Mike Marcolini, Head, Aeronautical Systems Analysis Branch, Dan Williams, Assistant Branch Head, Aeronautical Systems Analysis Branch and William Kimmel, Chief Technologist, Systems Analysis and Concepts Directorate; as well as the Fundamental Aeronautics Program office for funding this project. Test data, technical discussion and guidance from Alex Velicki, Dawn Jegley and Andrew Lovejoy are greatly appreciated.

IX. References

[1] Liebeck, R. H., "Configuration Control Document CCD-3: Blended Wing Body," Final report Under Contract NAS1-20275 NASA Langley Research Center, October 1997.
[2] Liebeck, R. H., Page, M. A., and Rawdon, B. K., "Blended-Wing-Body Subsonic Commercial Transport," AIAA Paper 1998-0438, January 1998.
[3] Liebeck, R. H, "Design of the Blended Wing Body Subsonic Transport," *Journal of Aircraft*, Vol. 41, No. 1, Jan-Feb. 2004, pp. 10-25.
[4] Hoffman, K., "Air Vehicle Technology Integration Program (AVTIP), Multi-role Bomber Structural Analysis, AFRL-VA-WP-TR-2006-3067, May 2006, Final Report for 14 December 2004 – 08 May 2006, AFRL-VA-WP-TR-2006-3067.
[5] Mukhopadhyay, V., "Structural Concepts Study of Non-circular Fuselage Configurations," Paper No. AIAA SAE WAC-67, World Aviation Congress, Los Angeles, Calif. Oct. 22-24, 1996.
[6] Mukhopadhyay, V., Sobieszczanski-Sobieski, J., Kosaka, I., Quinn, G., and Vanderplaats, G., "Analysis, Design and Optimization of Non-cylindrical Fuselage for Blended-Wing-Body Vehicle," *Journal of Aircraft*, Vol. 41, No. 4, July-August, 2004, pp. 925-930.
[7] Bradley, K. R., "A Sizing Methodology for the Conceptual Design of Blended-Wing-Body Transports, *MS Thesis, Joint Institute for Advancement of Flight Sciences, George Washington University*, Sep. 2004.
[8] Velicki, A, and Hansen, D., "Novel Blended Wing Body Structures Concepts," BWB-NNL04AA36C-CLIN; The Boeing Company, Phantom Works, Final Report, Sep. 2004.
[9]Velicki, A., Thrash, P. J., and Hawley, A.V., "Preliminary Design Requirements," Damage Arresting Composites for Shaped Vehicles," NASA Contract NNL07AA48C, Mid-term Report December 2007 and April 2008.
[10] Renton, J. W., Olcott, D., Roeseler B., Batzer, R., Baron, B., and Velicki, A., "Future of Flight Vehicle Structures (AIAA Paper 2002-2023)," *AIAA Journal*, Vol. 41, No. 51, 2004, pp. 995-998.
[11]Velicki, A., and Thrash, P. J., "Advanced Structural Concept Development Using Stitched Composites," The Boeing Company, Huntington Beach, California 92647-2099, AIAA Paper 2008-2329.
[12]Velicki, A., Thrash, P. J., and Jegley, D., "Airframe Development for the Hybrid Wing Body Aircraft," AIAA Paper 2009-932.
[13] Lovejoy, A. E., Rouse, M., Linton, K. A., and Li, V. P., "Pressure Testing of a Minimum Gauge PRSEUS Panel," AIAA-2011-1813, 52nd AIAA/ASME/ASCE/AHS/ASC Structures, Structural Dynamics, and Materials Conference, Denver, April, 2011.
[14] Yovanof , N. P. and Jegley, D.C., "Compressive Behavior of Frame-Stiffened Composite Panels," AIAA-2011-1913, 52nd AIAA/ASME/ASCE/AHS/ASC Structures, Structural Dynamics, and Materials Conference, Denver, April 2011.
[15] Velicki, A., Yovanof, N., Baraja, J., Linton, K., Li, V., Hawley, A., Thrash, P., DeCoux, S., and Pickell, R., "Damage Arresting Composites for Shaped Vehicles-Phase II Final Report, NASA/CR–2011-216880, 2011.
[16] Velicki, A., and Jegley, D., "PRSEUS Development for Hybrid Wing Body Aircraft, "11th AIAA Aviation Technology, Integration and Operations Conference, AIAA Centennial of Naval Aviation Forum, Virginia Beach, Virginia, 2011.
[17]Mukhopadhyay, V., "A Conceptual Aerospace Vehicle Structural System Modeling, Analysis and Design Process," AIAA Paper 2007-2372, April 2007.

[18] Mukhopadhyay, V: "Hybrid Wing-Body Pressurized Fuselage Modeling, Analysis, and Design for Weight Reduction," AIAA Paper 2012-1999, April 2012.
[19] Gern, F., "Improved Aerodynamic Analysis for Hybrid Wing Body Conceptual Design Optimization, AIAA-2012-0249, 50th AIAA Aerospace Sciences Meeting, January, 2012.
[20] Nickol, C., "Hybrid Wing Body Configuration Scaling Study," AIAA-2012-0337, 50th AIAA Aerospace Sciences Meeting, January, 2012.
[21] Gern, F. H., "Finite Element Based HWB Centerbody Structural Optimization and Weight Prediction, AIAA Paper 2012-1606, 53rd AIAA/ASME/ASCE/AHS/ASC Structures, Structural Dynamics, and Materials Conference, Honolulu, HI, April 2012.
[22] Gern, F., "Conceptual Design and Structural Analysis of an Open Rotor Hybrid Wing Body Aircraft," AIAA Paper Presented at the 54th AIAA/ASME/ASCE/AHS/ASC Structures, Structural Dynamics, and Materials Conference, Boston, April 2013.
[23]Laughlin, T., "A Parametric and Physics-Based Approach to Structural Weight Estimation of the Hybrid Wing Body (HWB) Aircraft," M.S. Thesis, Aerospace Engineering Dept., Georgia Institute of Technology, July 2012.
[24]Voet, Z. V., Gueskens, F., Ahmed, T. J., Eyben, B. N., and Beukers, A., "Configuration of the Multibubble Pressure Cabin in Blended Wing Body Aircraft," *J. Aircraft*, V.49, N.4, July-August 2012, pp.991-1007.
[25] Timoshenko, S., and Krieger, S.W., "*Theory of Plates and Shells*," *McGraw-Hill, New York*, 2nd Edition, 1959, pp.197-202, pp. 364-377.
[26]Timoshenko, S., and Gere, J.M, "*Theory of Elastic Stability," McGraw-Hill, New York, Reprinted by Dover, New York*, 2nd Edition, 1989, pp.1-45, pp.348--387.
[27] Paik, J. K., Thayamballi, A. K., and Kim, B. J., "Large Deflection Orthotropic Plate Approach to Develop Ultimate Strength Formulations for Stiffened Panels under Combined Biaxial Compression/Tension and Lateral Pressure," *Thin-Walled Structures,* Elsevier Publications (www.elsevier.com/locate/tws), Vol. 39, 2001, pp. 215–246.
[28]Shimpi, R. P., and Patel, H. G., "A Two Variable Refined Plate Theory for Orthotropic Plate Analysis," *ASME Journal of Applied Mechanics*, Vol. 55, 2004, pp.7783-6799.
[29] Hwang, I. and Lee, J. S., "Buckling of Orthotropic Plates under Various In-plane Loads," *KSCE Journal of Civil Engineering*, Vol. 10, No. 5, September 2006, pp. 349–356.
[30] SolidWorks and SolidWorks Simulation User Manual, *SolidWorks Corporation, Dassault Systèmes, Concord, Massachusetts*.

54th AIAA/ ASME/ ASCE/ AHS/ ASC Structures, Structural Dynamics, and Materials Conference
General Chair: Anthony M. Waas, Univ of Michigan, 734-764-8227 dcw@umich.edu
Technical Program Chair: Ajit K. Roy, Air Force Research Lab, 937-255-9034 ajit.roy@wpafb.af.mil

SESSION: Design Engineering. TC: Chair Jerry Brown, gerald.a.brown@boeing.com.
Design Engg. Editor: Russ Althof eralthof@raytheon.com
AIAA Deadline Abstract: September 7, 2012-Accepted Dec 19, 2012
NASA/TPSAS ID: 15273 (Approved September 7, 2012)
AIAA CONTROL ID: 1514922
TITLE: Hybrid Wing Body Pressurized Fuselage and Bulkhead Design and Optimization
AUTHORS (LAST NAME, FIRST NAME): Mukhopadhyay, Vivekanand[1]
INSTITUTIONS (ALL): 1. NASA Langley Research Center, Hampton, VA, United States.
PRESENTATION TYPE: Technical Paper
CURRENT TOPIC: 54th AIAA/ASME/ASCE/AHS/ASC Structures, Structural Dynamics, and Materials Conference
CURRENT SUB-TOPIC: Design Engineering: Advanced Aircraft; SDM-39 April 9, 2013 2-5 pm
KEYWORDS: AEROSPACE DESIGN & STRUCTURES: Design Engineering.
Abstract File Upload: SDM_2013_HWB_Abstract_Vivek_Final.pdf

54th AIAA/ASME/ASCE/AHS/ASC
Structures, Structural Dynamics and Materials (SDM) Conference
8-11 April 2013, Boston Park Plaza Hotel, Boston, Massachusetts

Session: SDM-39 Design Engineering: Advanced Aircraft. April 9, 2013 2-5pm
Extended Abstract (Aug. 31, 2012 TPSAS and AIAA Sep. 7, 2012 NASA/TPSAS ID: 15273**)**
AIAA Accepted Notification: Dec. 13, 2012
Control ID#: 1514922

54th AIAA/ASME/ASCE/AHS/ASC Structures, Structural Dynamics, and Materials Conference on Boston Massachusetts, USA.

The session specifics you will be presenting at are:
Session Title: Design: Advanced Aircraft
Session Chair: Gary A Honea <gahonea@raytheon.com>
Co-chair: Russ Althof, Raytheon
Session Abbreviation: SDM-39
Client Session ID: 76
Session Type: Paper
Session Topic: Structural Dynamics and Materials/SDM (Papers)
Session Day and Times: April 9, 2013 2:30 PM - 6:00 PM
Session Location: Charles River